Journal of Physical and Theoretical Chemistry
of Islamic Azad University of Iran, 13 (1) 35-59: Spring 2016
(J. Phys. Theor. Chem. IAU Iran)
ISSN 1735-2126

Theoretical study of tetrahedrane derivatives

Mehdi Nabati[1,*], Mehrdad Mahkam[1] and Yaser Gholizade Atani[2]

[1] Chemistry Department, Faculty of Science, Azarbaijan Shahid Madani University, Tabriz, Iran
[2] Mathematics Department, Faculty of Science, Azarbaijan Shahid Madani University, Tabriz, Iran

Received February 2016; Accepted May 2016

ABSTRACT

Tetrahedrane is most strained and the smallest cage compound. It attracts organic chemists because of its unusual bonding nature and highly symmetrical structure. However, many efforts to isolate the parent tetrahedrane have been unsuccessful because of the high reactivity and very short lifetime caused by the strain in this molecule. Modeling of molecules for determination of structural properties of them prior to synthesizing molecule in the laboratory is an important method. The computational chemistry is more completely in understanding a problem. In present study, the density functional theory (DFT-B3LYP) method with 6-31G (d) basis set was used for optimizing and studying the electronic structural and detonation properties of tetrahedrane derivatives at 298.15 K temperature and 1 atmosphere pressure. The results show the tetrahedrane system with more electron withdrawing groups will be deviated from standard and stable state. And also, the $–NHNH_2$, $-NHNO_2$, $-NO_2$ and $-ONO_2$ groups give the detonation property to the tetrahedrane system.

Keywords: Theoretical Study; Density Functional Theory; Tetrahedrane; Electrophilicity Iindex; Detonation Properties

INTRODUCTION

Tetrahedrane (tricycle [1.1.0.$0^{2,4}$]butane) is a most highly strained ring system with having a carbon framework demonstrated by the simplest connected cubic graph [1]. It is a very important and interesting system for novel high-tech compounds [2]. For more decades, scientists have been trying to prepare it [3]. Nevertheless, few derivatives of this compound such as tetrakis (trimethylsilyl) tetrahedrane has been synthesized as yet [4]. But, theoretically properties of this cage-like structure were discussed completely [5-7]. For determining structural properties of the molecules, modeling a molecular system prior to synthesizing molecule in the laboratory is an important method. The preparing a compound could need months of labor and raw materials, and generates toxic waste [8-12]. On the other hand, the computational chemistry is more completely in understanding a problem [13]. There are some properties of a molecule that can be obtained theoretically more easily than by experimental means [14]. Density functional theory (DFT) has become very popular in recent years. This is justified based on the pragmatic observation that it is less computationally intensive than other methods with similar accuracy [15,

*Corresponding author: mnabati@ymail.com

16]. In the present work, we are studied theoretically fifty two derivatives of tetrahedrane (-CH_3, -F, -CN, -OH, -COOH, -$CONH_2$, -NH_2, -$NHNH_2$, -$NHNO_2$, -NO_2, -NO, -ONO_2 and –N_3 substituents) by using quantum chemical treatment. All molecules properties were investigated at B3LYP/6-31G(d) level of theory. The B3LYP/6-31G(d) method is used for this reason that B.S. Jursic has introduced it as the best method for the tetrahedrane system in 2000 [17].

COMPUTATIONAL METHOD

All of our theoretical studies in this work were performed with the Gaussian 03 package [18] using the B3LYP method with 6-31G(d) basis set. The term of B3LYP consists of the Vosko, Wilk, Nusair (VWN3) local correlation functional [19] and Lee, Yang, Parr (LYP) correlation correction functional [20, 21]. The B3LYP/6-31G(d) was used as implemented in the Gaussian computational study. The geometry of structures was optimized without any structural or symmetry restrictions. The studied methods were used to predict the HOF of the molecule via atomization reaction. Vibrational analyses without any symmetry constraints were done for each set of calculations. Theoretical calculations have been performed in the gas phase [22]. To calculate the density of structures, the molecular volume data was required. The molecular volume V was defined as inside a contour of 0.001 electrons/bohr^3 density. The computational molecular density ρ (ρ=M/V, where M = molecular weight) was also calculated. The computational molecular density ρ (ρ=M/V, where M = molecular weight) was also calculated. Oxygen balance (OB_{100}) is an expression that is used to indicate the degree to which an explosive ($C_aH_bO_cN_d$) can be oxidized. OB_{100} was calculated as follows:

$$OB\% = \frac{-1600}{\text{Mol. wt}} \times \left(2a + \frac{b}{2} - c\right)$$

where: a = number of atoms of carbon, b = number of atoms of hydrogen, c = number of atoms of oxygen.

The atomization reactions method has been performed very successfully to calculate heat of formations (HOFs) using total energies obtained from density functional theory (DFT) calculations. The mathematical analysis of equations was carried out with Matlab® R2014a package [23].

RESULTS AND DISCUSSION

This section shows and discusses the results consisting the geometry, Mulliken atomic charges, frontier orbitals energy, electrophilicity, heat of formation (HOF), detonation properties, thermal stability and natural bond orbitals (NBOs) for all structures at the B3LYP/6-31G(d) level of theory.

The Geometry of the Structures

We were computed successfully the structural properties of tetrahedrane system derivatives (Scheme 1) with DFT methods at 293.15 K and 1 atmosphere. The geometric structure of the studied molecule is showed in Figure 1. We have seen whatever the number of withdrawing groups on the tetrahedrane system increases, the structure will be destroyed and converted into the cyclobutene and cyclobutadiene. The Mulliken atomic charges of the molecules at studied level of theory are listed in Table 1. As seen from the data, the carbon atoms attached to the substituents and the carbon atoms attached to hydrogen have positive and negative charges, respectively. This factor makes the covalent $\sigma_{C\text{-}C}$ bonds find small ionic property. Then, the tetrahedrane system with more electron withdrawing groups will

be deviated from standard and stable state. This effect is more visible in the composition H1. For this reason, it is most unstable structure.

The Frontier Molecular Orbital Energies of the Structures

Table 2 shows the HOMO and LUMO energies (ε) of the molecule computed at the B3LYP/6-31G(d) level of theory. Density functional theory (DFT) methods have many important applications to chemistry. In DFT methods, two important parameters, the electronic chemical potential μ and the absolute hardness η help us to characterize chemical systems. The electronic chemical potential (the negative of the electronegativity, $-\chi = \mu$) is a thermodynamic measure of the electron tendency to scarper from the electron cloud, and is pertained to both electronic affinity and ionization potential characters. The global hardness η is defined as a feature that branched from the μ. The hardness η is a measure of the structures resistance to a change in its electronic configuration. If $\eta > 0$, the stability increases and the reactivity of the species decreases. In other words, the charge transfer process is energetically adjutant [24]. The ionization energy and electron affinity can be tabernacle by the frontier molecular orbitals HOMO and LUMO energies, respectively ($I = -\ \varepsilon_{HOMO}$ and $A = -\ \varepsilon_{LUMO}$) [25]. The electronic chemical potential is half-way between the HOMO and the LUMO on the energy scale. The gap of the HOMO and the LUMO energies is equal to 2η (both the electronic chemical potential and the hardness are measured in electron-volts). Electron transfer between reactants occurs between the molecular orbitals of HOMO and LUMO. The index ω is defined as electrophilicity character that measures the energy stabilization when the system obtains an additional electronic charge from the environment. So, we can acquire the reactivity indexes such as μ, η and ω from frontier orbitals energies by following equations:

$$\mu\ (\text{eV}) = -\frac{(\text{ELUMO} + \text{EHOMO})}{2}$$

$$\eta\ (\text{eV}) = \text{ELUMO} - \text{EHOMO}$$

$$\omega\ (\text{eV}) = \frac{\mu 2}{2\,\eta}$$

The index ω denotes electrophilicity power 1.62, 2.06, 1.52, 1.72, 1.64, 1.59, 1.22, 1.17 and 1.31 for C_2H_2, C_2HF, BH_3, HNO_3, CS_2, C_4H_4, Azulene, Anthracene and Perylene respectively [26]. In this study, index ω value of the structures has been calculated by the application of density functional theory using B3LYP/6-311G(d) basis set (Table 2). From the data, it is obtained that the molecules have low electrophilicity. And also, whatever the number of groups on the tetrahedrane system increases, index ω value of the structures is larger.

Predicted Heat of Formations (HOFS), Densities and Detonation Properties of the Structures

The heat of formation (HOF) of a compound is the change of enthalpy from the formation of 1 mole of the compound from its constituent elements, with all substances in their standard states at 1 atmosphere [27]. The HOF values of the studied structures were calculated at B3LYP/6-31G(d) level of theory and listed in the table 3. In the present study, atomization reaction method is employed for calculation of HOFs. Because of high strained geometry of the tetrahedrane structure, there is a detonation effect possible for the compounds. Then, important parameters of a detonation compound ($C_aH_bO_cN_d$) such as density (ρ), detonation velocity (D), and detonation pressure (P) can be predicted by the empirical Kamlet–Jacobs equations [28] as follows:

	Stoichiometric ratio		
parameters	c≥2a+b/2	2a+b/2□c≥b/2	b/2□c
N	(b+2c+2d)/4MW	(b+2c+2d)/4MW	(b+d)/2MW
M	4MW/(b+2c+2d)	(56d+88c-8b)/(b+2c+2d)	(2b+28d+32c)/(b+d)
Q	(28.9b+94.05a+0.239ΔHf□)/MW	[28.9b+94.05(c/2-b/4)+0.239ΔHf□]/MW	(57.8c+0.239ΔHf□)/MW

$$D=1.01(NM^{1/2}Q^{1/2})^{1/2}(1+130\rho)$$
$$P=1.558\rho^2NM^{1/2}Q^{1/2}$$

where D: detonation velocity in km/s, P: detonation pressure in GPa, ρ: density of a compound in g/cm^3, N: moles of gaseous detonation products per gram of explosive (in mol/g), M: average molecular weight of gaseous products (in g/mol), Q: chemical energy of detonation in kJ/g. Table 2 collects the predicted V, ρ, Q, D and P of the structures. The structures density was computed from the molecular volume, while the molecular volume for each structure was gained from the statistical average of 100 single-point calculations for optimized compound. The molar volume was defined as inside a contour of 0.001 e/Bohr^3 density that was evaluated using a Monte Carlo integration implemented in the Gaussian 03 package. For RDX and HMX, experimental value of D and P are 8.75 km/s, 9.10 km/s and 34.70 GPa, 39.00 GPa, respectively [29]. The RDX and HMX are the current standards for detonation behavior [30]. Comparing these values with tetrahedrane derivatives, H1 (has detonation velocity value of 11.393 km/s and detonation pressure value of 46.429 GPa), H3 (has detonation velocity value of 10.14 km/s and detonation pressure value of 47.199 GPa), I2 (has detonation velocity value of 9.654 km/s and detonation pressure value of 45.534 GPa), I3 (has detonation velocity value of 9.237 km/s and detonation pressure value of 39.743 GPa), I4 (has detonation velocity value of 9.792 km/s and detonation pressure value of 46.395 GPa), J3 (has detonation velocity value of 9.333 km/s and detonation pressure value of 41.321 GPa), J4 (has detonation velocity value of 10.03 km/s and detonation pressure value of 49.743 GPa), L1 (has detonation velocity value of 8.886 km/s and detonation pressure value of 37.841 GPa), L3 (has detonation velocity value of 10.532 km/s and detonation pressure value of 57.706 GPa), shows them to be more powerful explosives than the standard explosives HMX and RDX.

The Effect of Substituent on the Electrophilicity Power

Figure 2 shows a comparison of the ω values for the tetrahedrane derivatives by the number of substituents. The tetrahedrane derivatives have different electrophilicity index values, for example, the largest and the smallest values are 0.24388 (K4) and 0.00159 (H1) a.u., respectively. As seen from the Table 2 and Figure 2, the ω index values increase by substituent numbers increasing (n: 4>3>2>1). And also, it can be deduced that the substituent effect order on tetrahedrane system electrophilicity power may be in the order of K>J>L>I>D>E>M>F>C>B>G>H>A. In other words, the electron withdrawing substituents increase the ω index.

The Effect of Substituent on the Hof

Figure 3 shows a comparison of the heat of formation values for the studied molecules by the number of substituents. The tetrahedrane derivatives have different HOF values, for example, the largest and the smallest values are 5204.243 (H1) and -1324.512 (E4) kJ/mol, respectively. As seen from the data (Table 3), the HOF values of the A, B, C, E, F, I, J, L series

increase by decreasing the number of substituents (n: 1>2>3>4). In series of D, M, K the HOF values increase by substituent numbers increasing (n: 4>3>2>1). The HOF values of the G and H series increase by the order of n: 3>4>2>1 and n: 1>3>4>2, respectively. These results indicate that the HOF parameter isn't related to the electronic and spatial effects of the substituents. As seen from the Figure 3, the H1 molecule has maximum value of the HOF between all structures. The Mulliken atomic charges data (Table 1) shows the large gap of the charges in σ-(C_H-C_{NHNH2}) bond of this molecule. This factor makes the covalent bond finds small ionic property. For this reason, it is most unstable structure. Comparing NBO analysis (Table 4) of the H1 with tetrahedrane and H2 shows this molecule uses from less amount of p orbital in C_H-C_{NHNH2} hybrid. Since we know the bonds in cage compounds use from more value of p orbital, then this makes the structure unstable. We can be deduced the HOF parameter is related to the type and hybrid of bonds.

The Effect of Substituent on the Heat of Explosion (Q)

Figure 4 shows a comparison of the Q values for the tetrahedrane derivatives by the number of substituents. The tetrahedrane derivatives have different heat of explosion values, for example, the largest and the smallest values are 15158.647 (H1) and 148.211 (B4) kJ/g, respectively. As seen from the data (Table 3), the Q values of the A, B, C, D, E, F, G, H, I, J, L series increase by decreasing the number of substituent (n: 1>2>3>4). The Q values of the K and M series increase by the order of n: 1>2>4>3 and n: 1>4>2>3, respectively. It can be deduced that the heat of explosion value is related to the geometry of the molecules. Whatever the original structure of the tetrahedrane backbone remains intact, the molecule is under more pressure and is unstable. Then the heat of explosion of it is more. As seen from the Figure 4, the H1 molecule has maximum value of the Q between all structures. As mentioned above, this molecule is unstable because of the type and the hybrid of bonds.

The Effect of Substituent on the Density of Explosion (ρ)

Figure 5 shows a comparison of the ρ values for the tetrahedrane derivatives by the number of substituents. The tetrahedrane derivatives have different density of explosion values, for example, the largest and the smallest values are 2.484 (B3) and 0.922 (A3) g/cm^3, respectively. As seen from the data (Table 3), the ρ values of the structures randomly change by increasing the number of substituents.

The Effect of Substituent on the Velocity of Detonation (D)

Another main property for the explosives is velocity of detonation (D). Figure 6 shows a comparison of the velocity of detonation values for the tetrahedrane derivatives by the number of substituents. The tetrahedrane derivatives have different D values, for example, the largest and the smallest values are 11.393 (H1) and 1.587 (B3) km/s, respectively. It is obtained from Figure 6, the velocity of datonation values of the molecules randomly change by increasing the number of substituents. As seen from the data (Table 3), the detonation velocity of structures H1, H3, I2, I3, I4, J3, J4, L1 and L3 is more than RDX. In other words, the –$NHNH_2$, -$NHNO_2$, -NO_2 and -ONO_2 groups give the detonation property to the tetrahedrane system. It can be deduced, the velocity of detonation property is related to the geometry of structures and type of the substituents.

The Effect of Substituent on the Pressure of Explosion (P)

A main parameter for the explosives is pressure of explosion (P). Figure 7 shows a comparison of the pressure of explosion values for the tetrahedrane derivatives by the number of substituents. The tetrahedrane derivatives have different P values, for example, the largest and the smallest values are 57.706 (L3) and 1.328 (B3) km/s, respectively. It is obtained from Figure 7, the pressure of explosion values of the molecules randomly change by increasing the number of substituents. As seen from the data (Table 3), the pressure of explosion of structures H1, H3, I2, I3, I4, J3, J4, L1 and L3 is more than RDX. In other words, the -$NHNH_2$, -$NHNO_2$, -NO_2 and -ONO_2 groups give the detonation property to the tetrahedrane system. It can be deduced, the pressure of explosion property is related to the geometry of structures and type of the substituents.

Comparison of Velocity of Detonation of the Structures by Electrophilicity Index Values

Every polynomial of degree 3 has some important points such as extermum point and inflection point. These points give us important information about the behavior of polynomial's graph. On the other hand, since using of polynomial is very simple, we approximate data with polynomial. In this section, we approximate data which were obtained in the Table 3 with polynomial of degree 3. Then according to the approximation polynomial, we consider about behavior of data around critical points. By approximating the data set (Table 3) with a polynomial of degree 3, we have:

$$y = -784.39x^3 + 204.4x^2 + 6.4112x + 5.7606$$

Figure 8 shows a comparison of the velocity of detonation values for the tetrahedrane derivatives by the electrophilicity indexes. As seen from the Figure 8, there are some critical points. If we compute the first and second derivatives of D-ω equation, we can obtain theoretical points. The first and second derivatives are obtained as following:

$$\frac{dy}{dx} = -2353.17x^2 + 408.8x + 6.4112$$

$$\frac{d^2y}{dx^2} = -4706.34x + 408.8$$

Figures 9 and 10 show the graphs of the first and second derivatives, respectively. The first derivative has two roots -0.0145, 0.1882 and the second derivative has one root 0.0869. However, we have two critical points 0.1882 and 0.0869 in the interval [0, 0.25]. So, the graph of D-ω has one extermum point at 0.1882 and one inflection point at 0.0869. Because of sign of second derivative at 0.1882 which is negative, so the velocity of detonation is maximum at this point, i.e. the structures have maximum velocity of detonation in this case. In other words, the velocity of detonation increases in the interval [0, 0.1882] and then decreases in the interval [0.1882, 0.25]. According to the inflection point 0.0869, we can say the increasing rate of velocity of detonation grows up in the interval [0, 0.0869] and drops in the interval [0.0869, 0.1882]. However, the velocity of detonation increases from 0 to 0.0869 faster than from 0.0869 to 0.1882, then, the velocity of detonation reduces after critical point 0.1882.

Comparison of Pressure of Explosion of the Structures by Electrophilicity Index Values

Similarly data set D-ω, the data set P-ω can be approximated by a polynomial of degree 3 as following:

$$y = -7499x^3 + 2061.7x^2 - 0.0869x + 14.73$$

Figure 11 shows a comparison of the pressure of explosion values for the tetrahedrane derivatives by the electrophilicity indexes. By computing the first and second derivatives of P-ω equation, we have:

$$\frac{dy}{dx} = -22497x^2 + 4123.4x - 0.0869$$
$$\frac{d^2y}{dx^2} = -44994x + 4123.4$$

Figures 12 and 13 show the graphs of the first and second derivatives, respectively. One can find extermum and inflection points of P-ω equation by computing roots of its first and second derivatives, respectively. The roots of the first derivative equation are 0.1833, -0.000 and the root of second derivative equation is 0.0916. The root -0.000 is not in the interval [0, 0.27], so we have one extermum point at 0.1833 and inflection point at 0.0916. As we can see from the Figure 11, the structures have maximum pressure of explosion at point 0.1833. In other words, in the interval [0, 0.1833] the pressure of explosion increases and after point 0.1833 decreases. Because of inflection point 0.0916 is contained in the interval [0, 0.1833], so we can consider about the increasing rate of pressure of explosion in this interval. The increasing rate of pressure of explosion grows up in the interval [0.0916, 0.1833], i.e. the pressure of explosion increases before point 0.0916 faster than after point 0.0916.

Comparison of Pressure of Explosion of the Structures by Oxygen Balance Values

By approximating the data set P-OB_{100}, the following polynomial of degree 3 can be obtained.

$$y = 2 \times 10^{-6}x^3 + 0.0011x^2 + 0.2639x + 39.249$$

The first and second derivatives of this equation can be computed easily as following:

$$\frac{dy}{dx} = 6 \times 10^{-6}x^2 + 0.0022x + 0.2639$$
$$\frac{d^2y}{dx^2} = 1.2 \times 10^{-5}x + 0.0022$$

Figures 14, 15 and 16 show the graphs of the P-OB_{100} equation, first and second derivatives, respectively. As Figure 15 shows, the first derivative of the P-OB_{100} equation doesn't have real roots. However, that has two complex roots -183.33±101.84i. Since there is no real roots for first derivative, so the pressure of explosion doesn't have any maximum at interior points of interval [-350, 50]. In other words, the pressure of explosion increases through the interval [-350, 50]. On the other hand, the second derivative equation has one real root -183.3333. This root shows that the increasing rate of pressure of explosion can be changed through the interval [-350, 50]. The Figure 15 shows the increasing rate of pressure of explosion drops before inflection point -183.3333 and then grows up after it.

Comparison of Velocity of Detonation of the Structures by Oxygen Balance Values

We can approximate data set D-OB_{100} by the following polynomial of degree 3:

$$y = 3 \times 10^{-7}x^3 + 0.0001x^2 + 0.0312x + 8.9872$$

Figure 17 shows a comparison of the velocity of detonation values for the tetrahedrane derivatives by the oxygen balance values. By computing the first and second derivatives of D-OB_{100} equation, we have:

$$\frac{dy}{dx} = 9 \times 10^{-7}x^2 + 0.0002x + 0.0312$$

$$\frac{d^2y}{dx^2} = 1.8 \times 10^{-6}x + 0.0002$$

Figures 18 and 19 show the graphs of the first and second derivatives, respectively. Since the first derivative equation has two complex roots -111.11±149.40i and its sign is positive, so the velocity of detonation which is approximated by D-OB_{100} equation, just increases through the interval [-350, 50]. In other words, we can't find any maximum point for velocity of detonation at the interior points of interval [-350, 50]. But according to the second derivative equation, there is one inflection point. This inflection point is -111.1111. Since the sign of second derivative is negative before inflection point and positive after this point. The first derivative equation is minimum at -111.1111, we can say increasing rate of velocity of detonation decreases in the interval [-350, -111.1111] and then increases in the interval [-111.1111, 50].

CONCLUSION

In the present work, structural properties of the tetrahedrane derivatives have been investigated theoretically by using quantum chemical treatment. Full geometrical optimization of the structures was performed using density functional theory (DFT, B3LYP) at the level of 6-31G(d). According to the results, we can be concluded as follows:

a. The tetrahedrane system with more electron withdrawing groups will be deviated from standard and stable state.

b. Whatever the number of groups on the tetrahedrane system increases, electrophilicity index (ω) value of the structures is larger.

c. The $–NHNH_2$, $-NHNO_2$, $-NO_2$ and $-ONO_2$ groups give the detonation property to the tetrahedrane system.

d. The electron withdrawing substituents increase the electrophilicity index.

e. The HOF parameter is related to the type and hybrid of bonds.

f. The heat of explosion value is related to the geometry of the molecules.

g. The ρ (density) values of the structures randomly change by increasing the number of substituents.

h. The velocity of detonation and the pressure of explosion properties are related to the geometry of structures and type of the substituents.

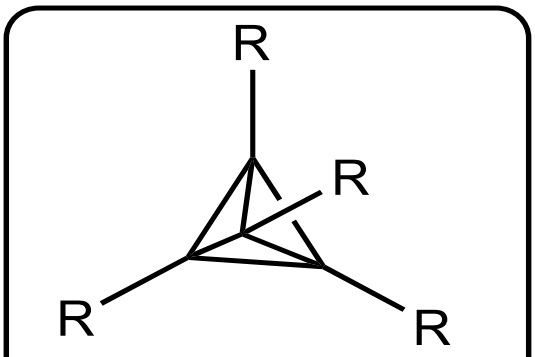

Tetrahedrane: R = H

An: $R_n = CH_3$, Bn: $R_n = F$

Cn: $R_n = OH$, Dn: $R_n = CN$

En: $R_n = COOH$, Fn: $R_n = CONH_2$

Gn: $R_n = NH_2$, Hn: $R_n = NHNH_2$

In: $R_n = NHNO_2$, Jn: $R_n = NO_2$

Kn: $R_n = NO$, Ln: $R_n = ONO_2$

Mn: $R_n = N_3$, n = 1, 2, 3, 4

Scheme 1. The structures of tetrahedrane derivatives.

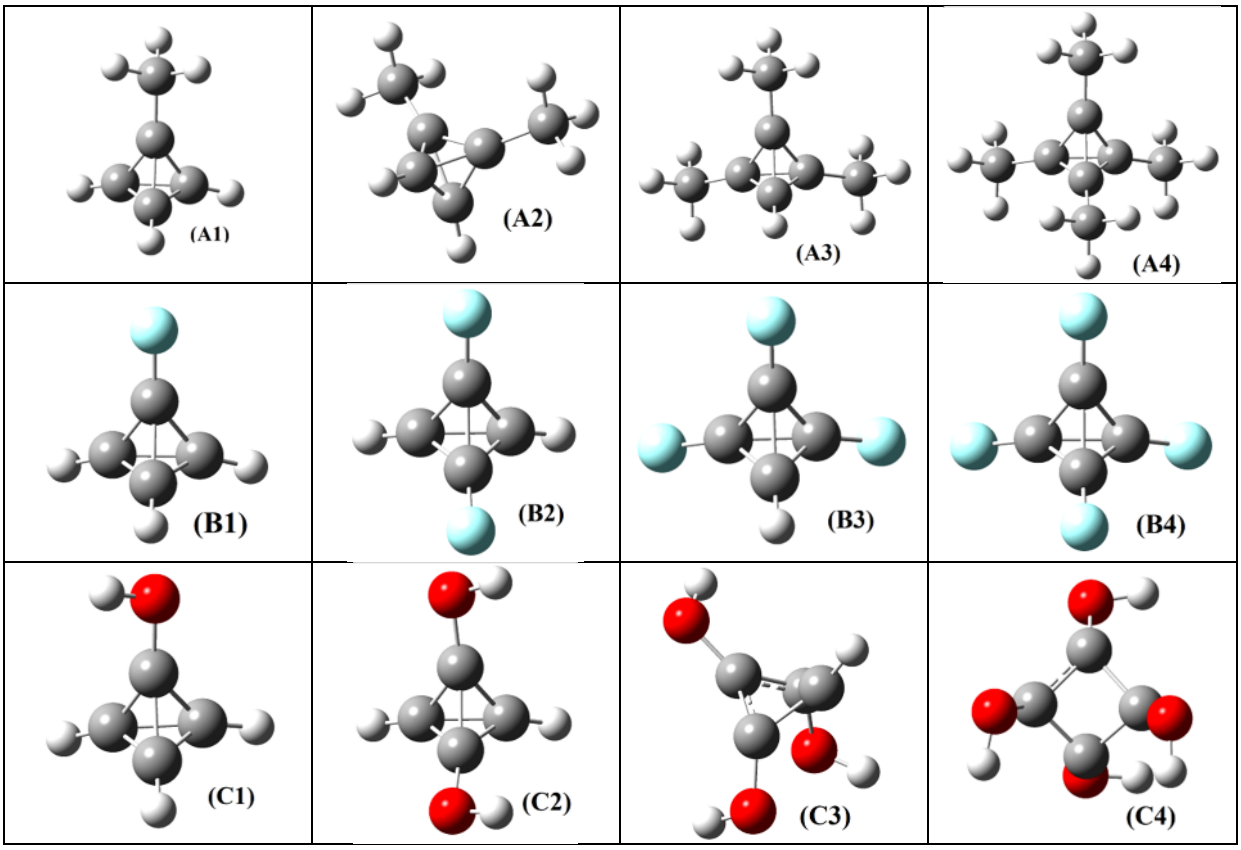

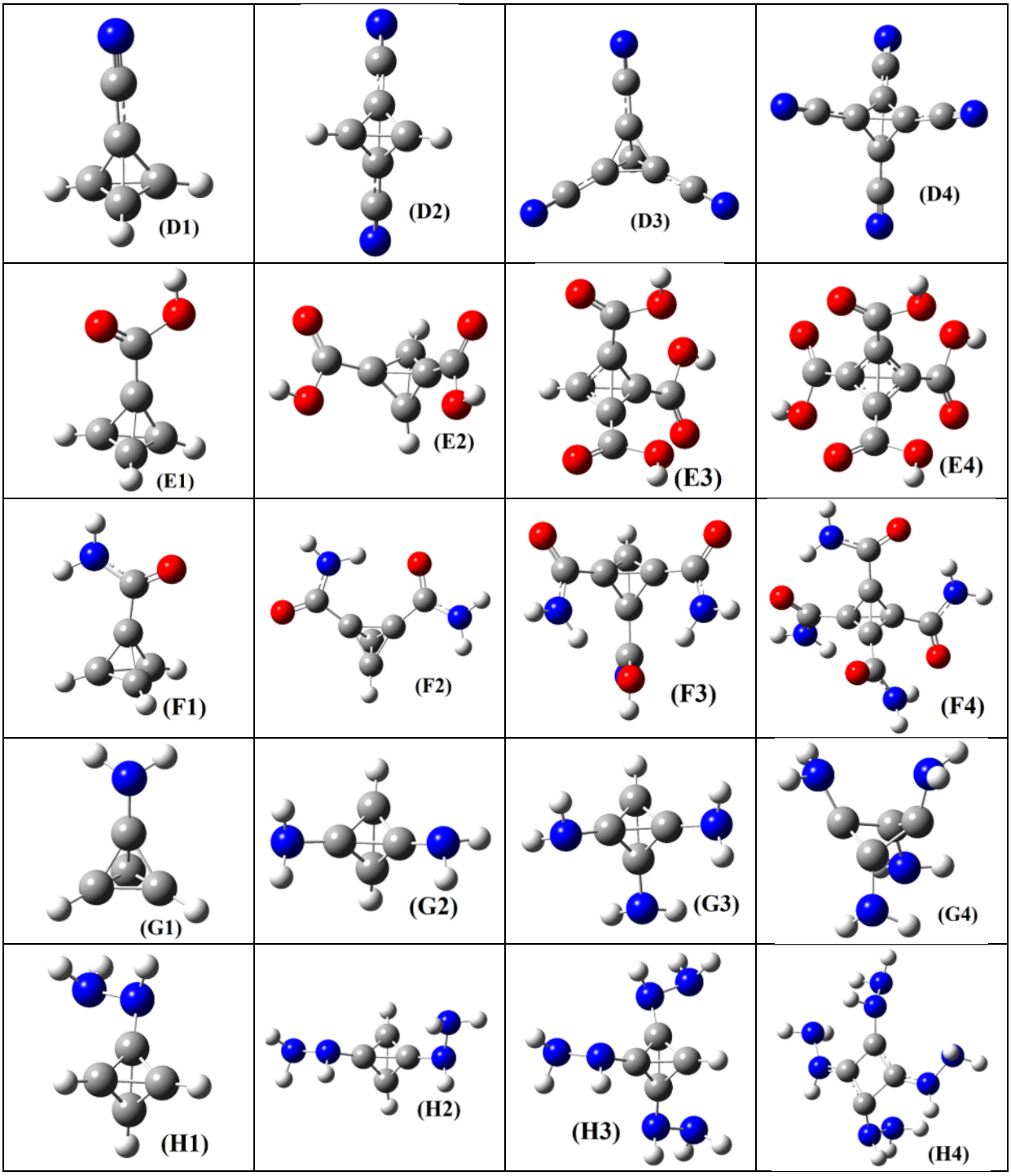
(D1)
(D2)
(D3)
(D4)
(E1)
(E2)
(E3)
(E4)
(F1)
(F2)
(F3)
(F4)
(G1)
(G2)
(G3)
(G4)
(H1)
(H2)
(H3)
(H4)

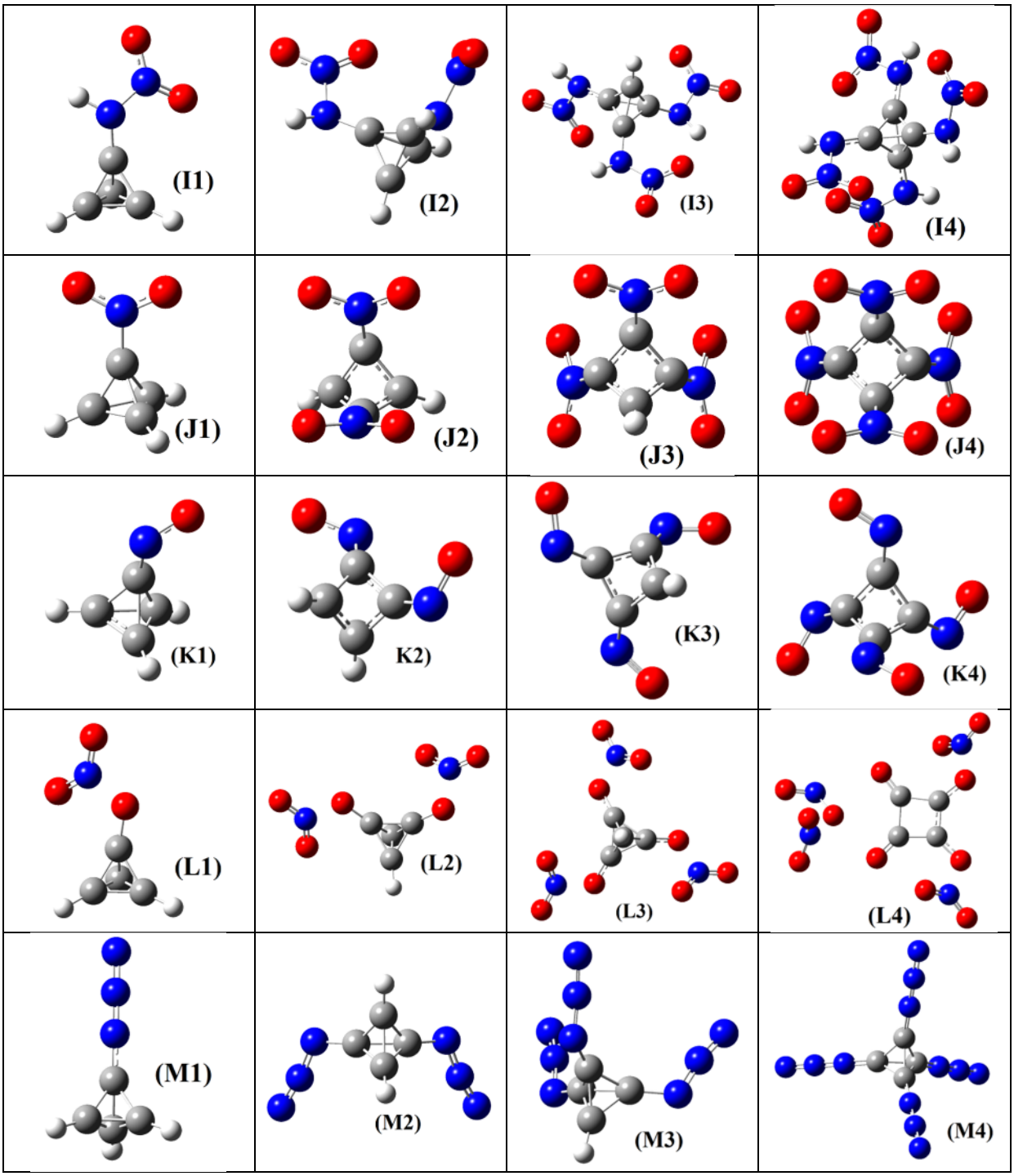

Fig. 1. The optimized geometry of the structures.

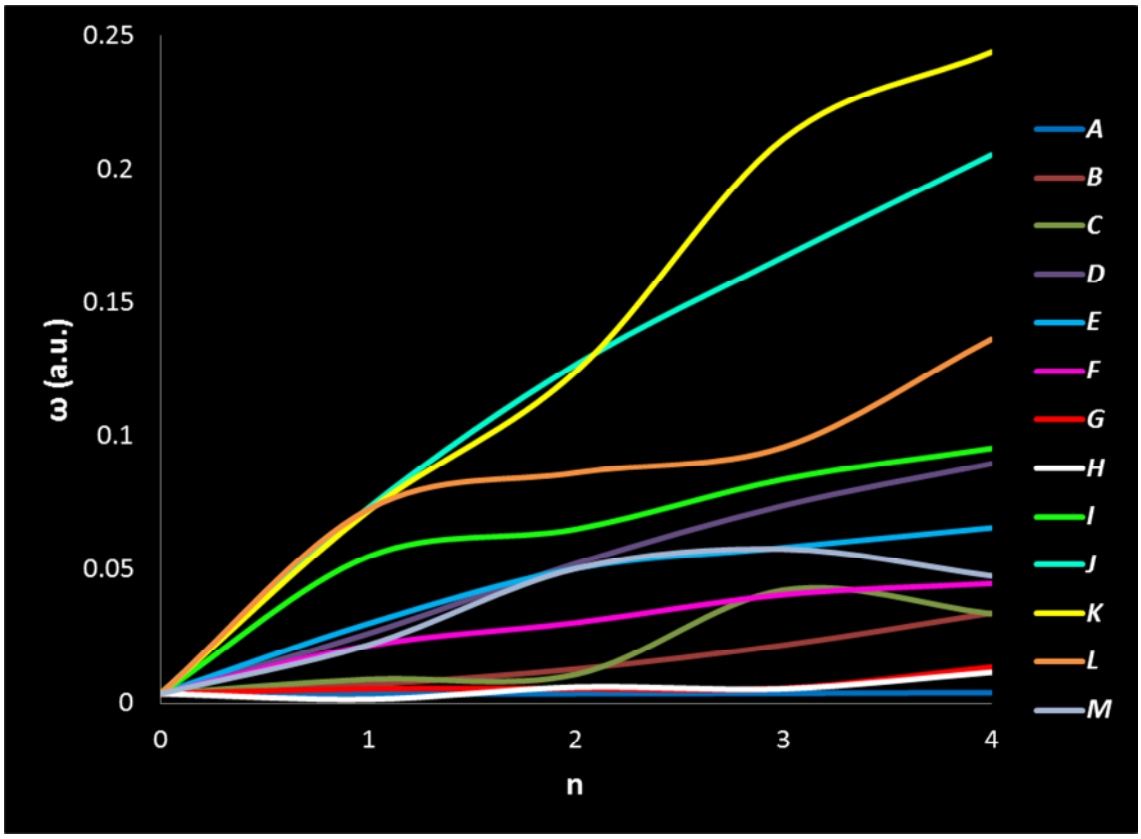

Fig. 2. Comparison of the electrophilicity indexes of the tetrahedrane derivatives influenced by the type and number of substituents.

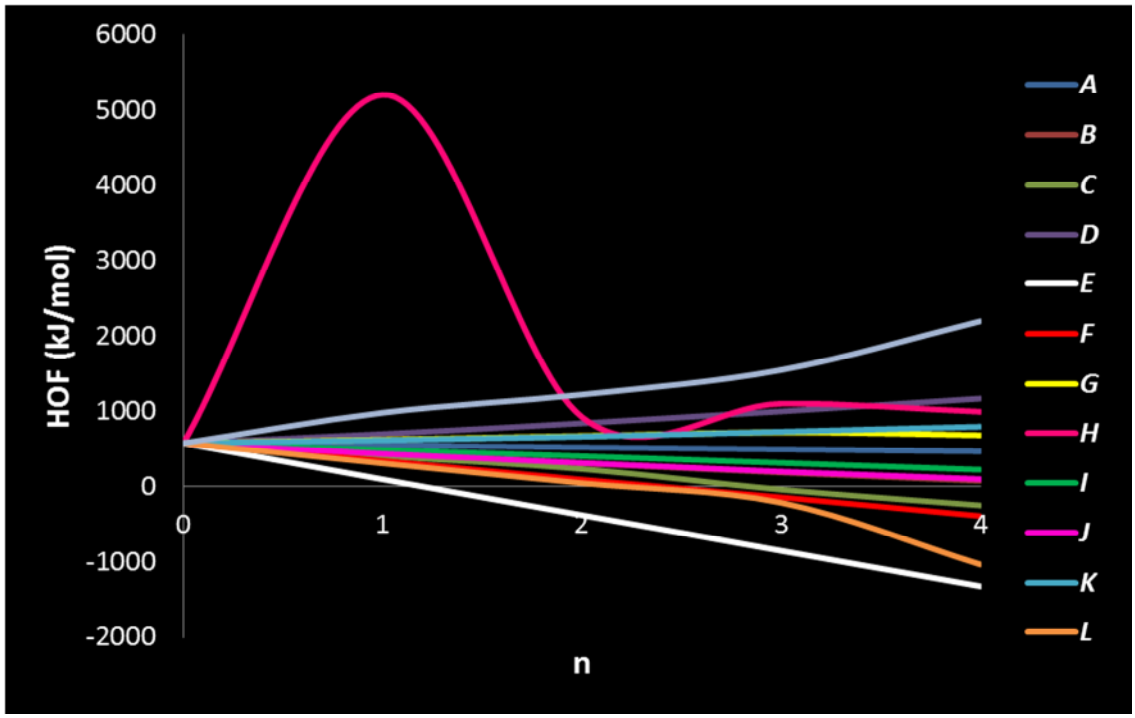

Fig. 3. Comparison of the HOFs of the tetrahedrane derivatives influenced by the type and number of substituents.

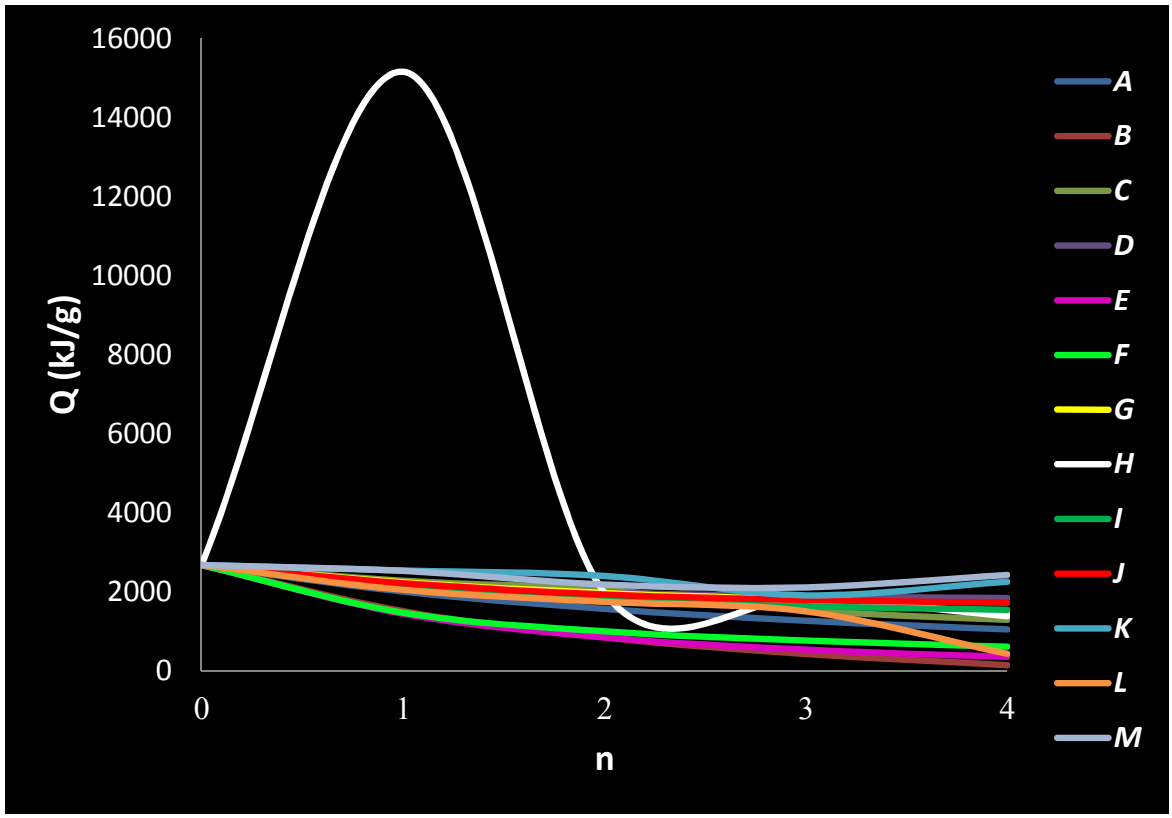

Fig. 4. Comparison of the Q values of the tetrahedrane derivatives influenced by the type and number of substituents.

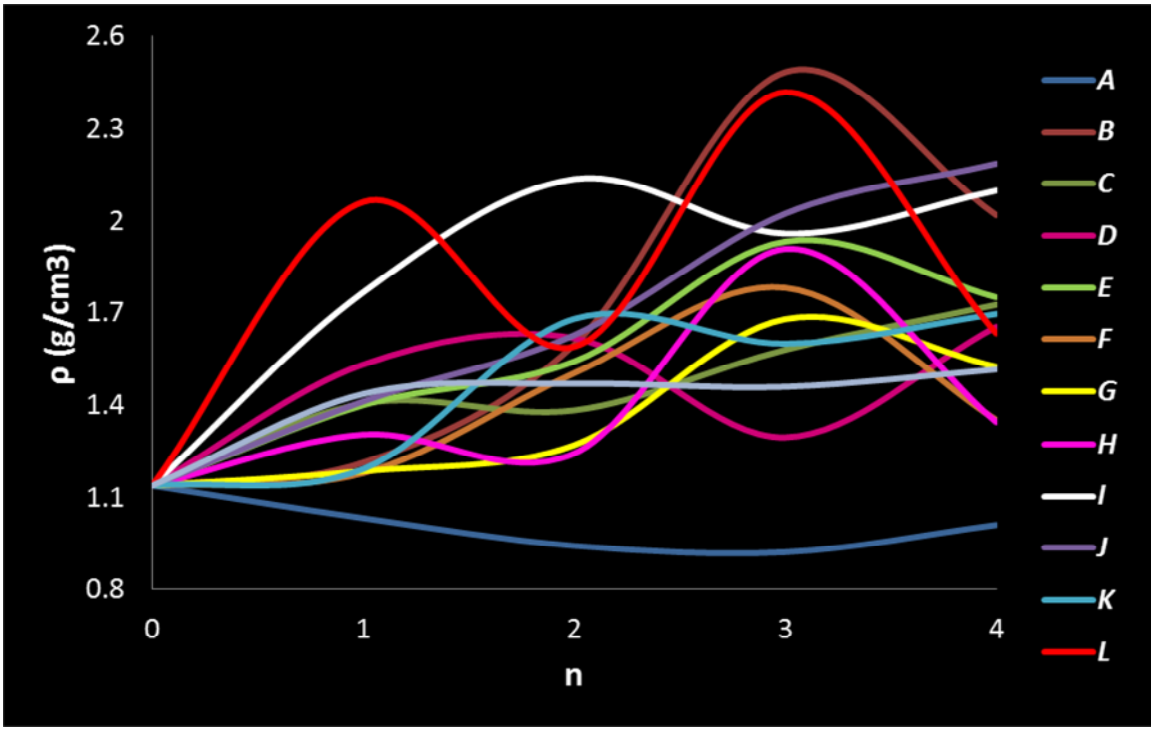

Fig. 5. Comparison of the ρ (density) values of the tetrahedrane derivatives influenced by the type and number of substituents.

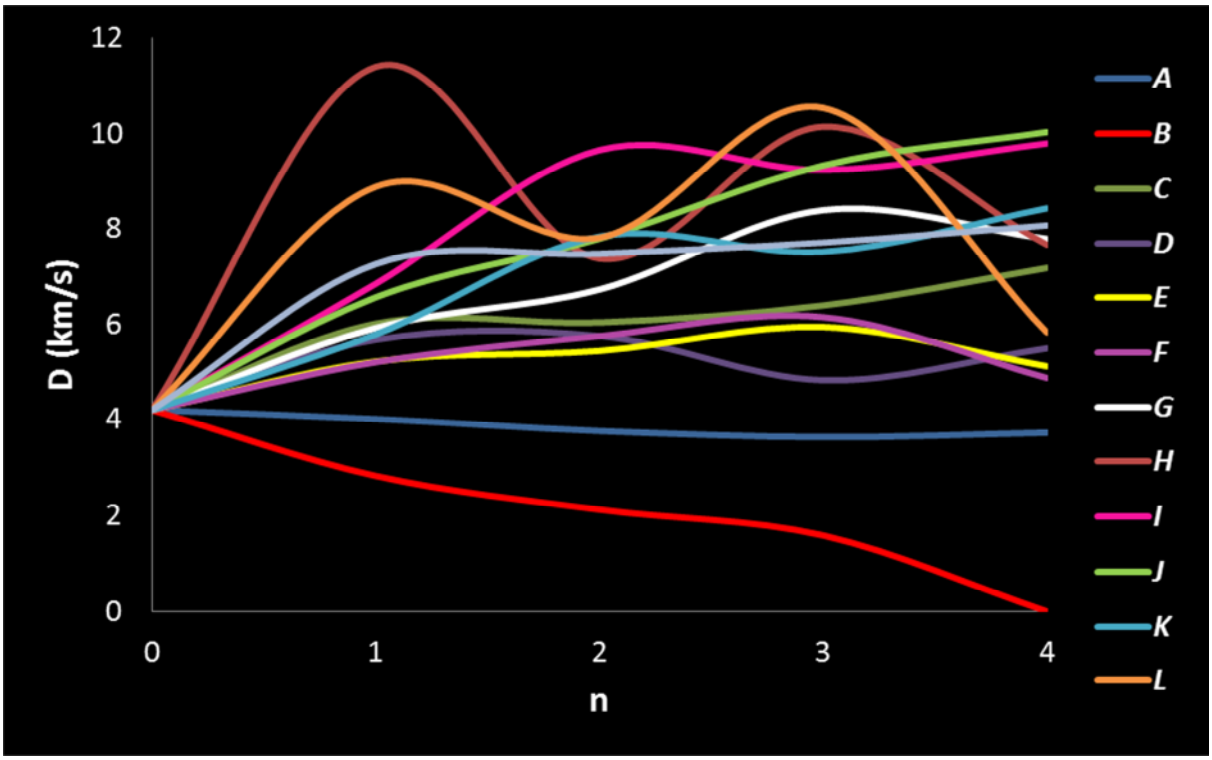

Fig. 6. Comparison of the D (velocity of detonation) values of the tetrahedrane derivatives influenced by the type and number of substituents.

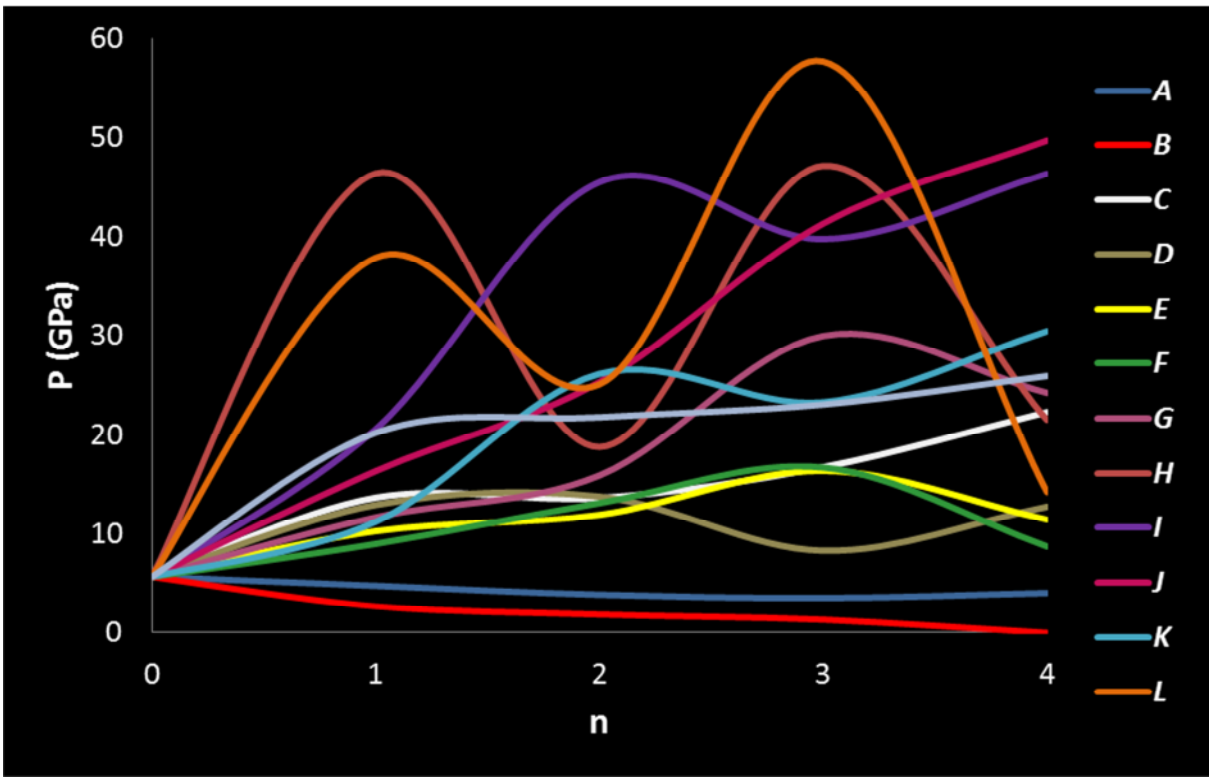

Fig. 7. Comparison of the P (pressure of detonation) values of the tetrahedrane derivatives influenced by the type and number of substituents.

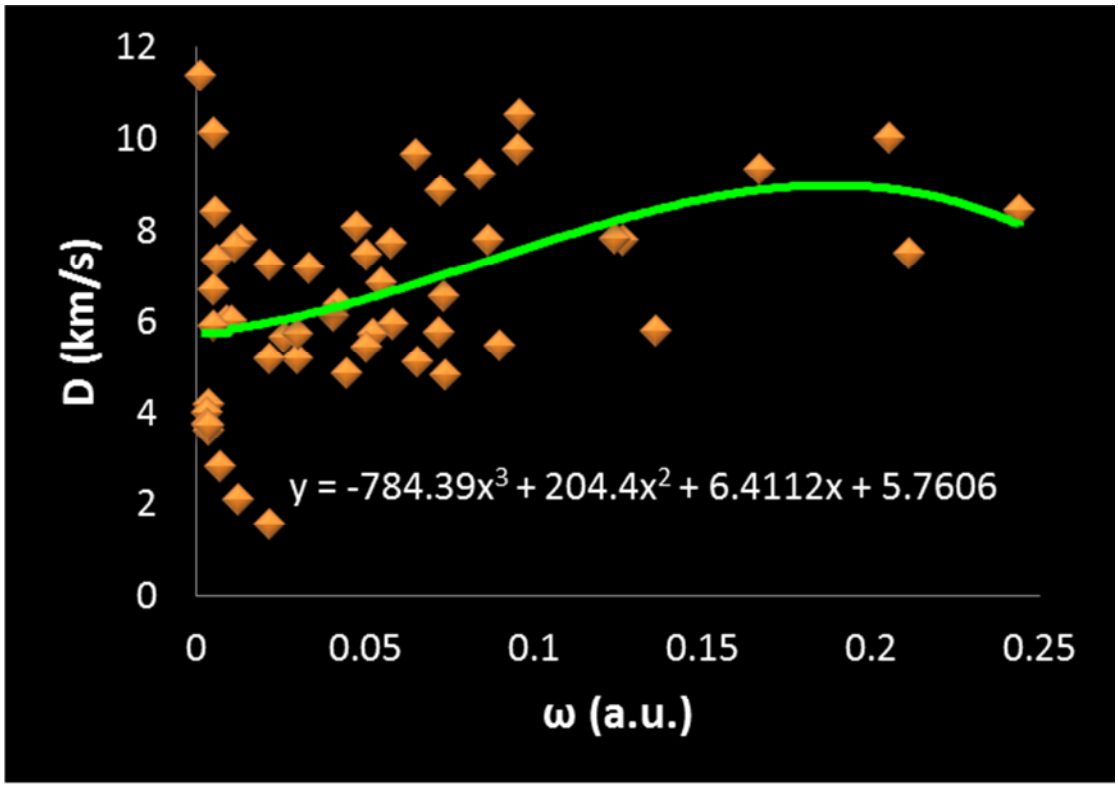

Fig. 8. Comparison of the D (velocity of detonation) values of the tetrahedrane derivatives influenced by the electrophilicity index of substituents.

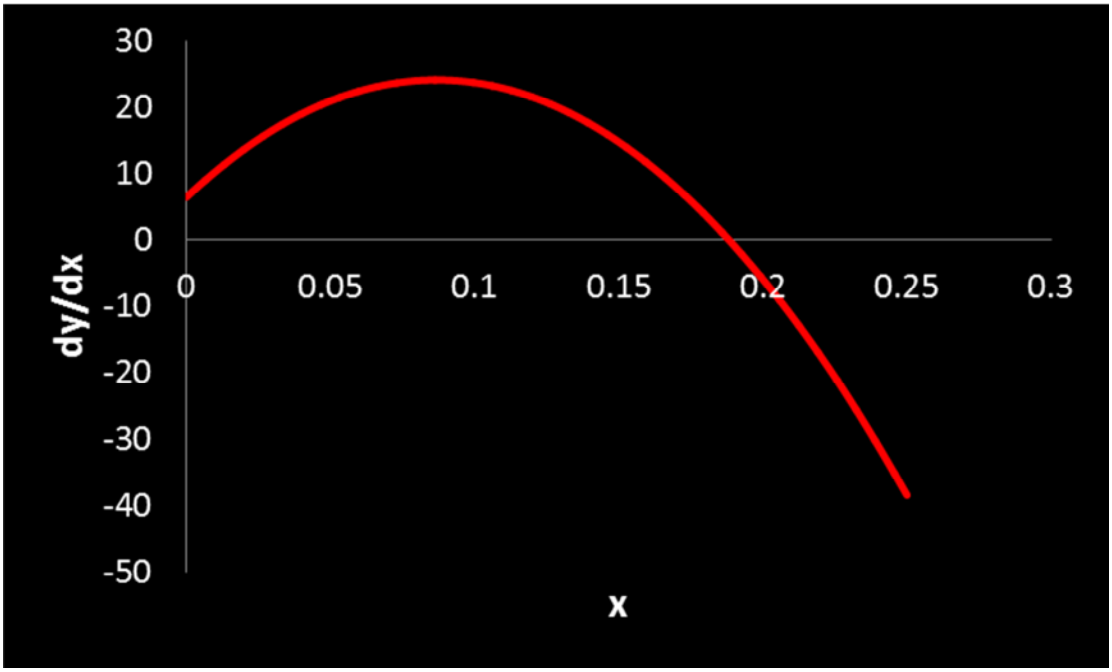

Fig. 9. First derivative of D-ω equation.

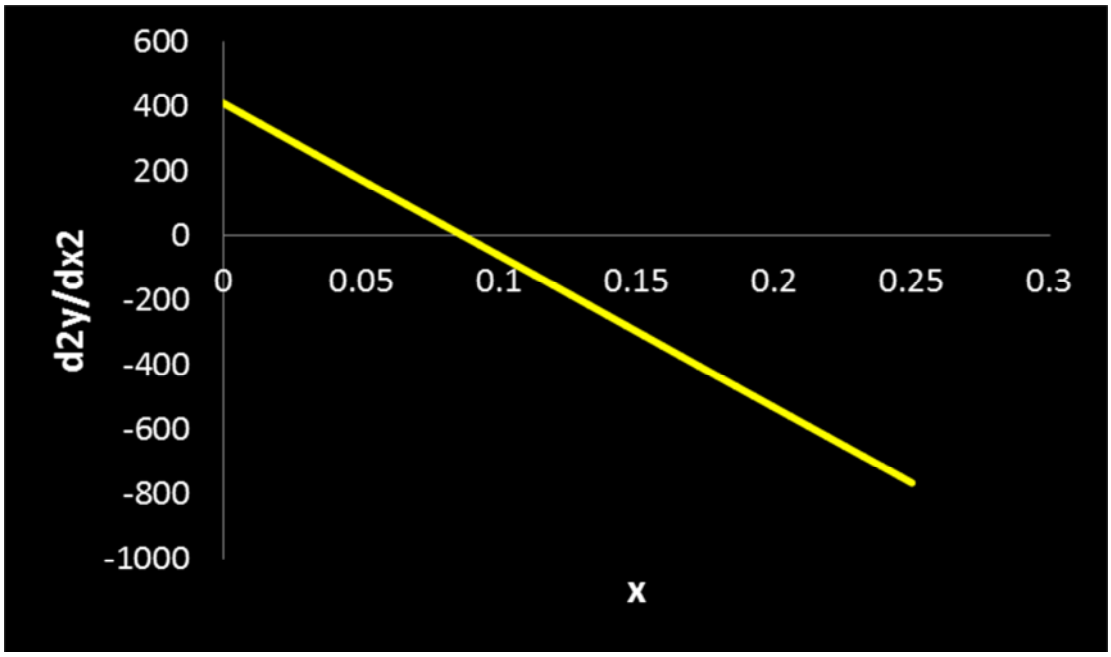

Fig. 10. Second derivative of D-ω equation.

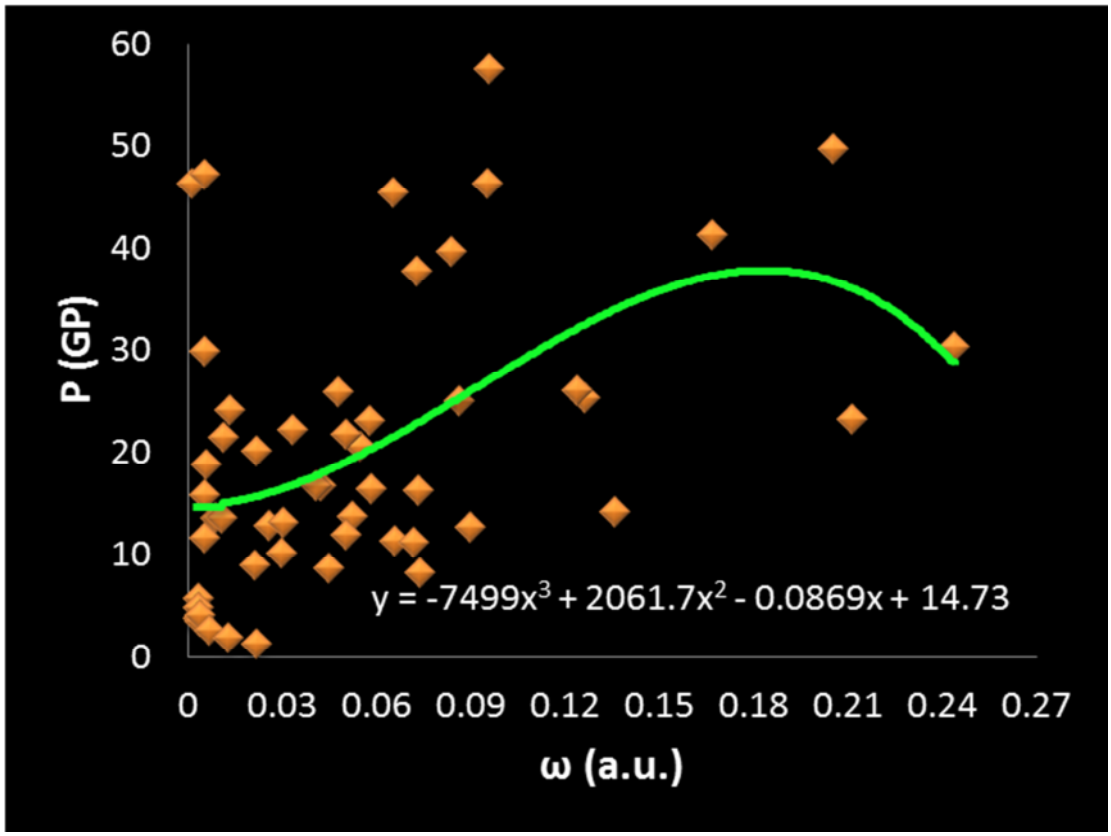

Fig. 11. Comparison of the P (pressure of detonation) values of the tetrahedrane derivatives influenced by the electrophilicity index of substituents.

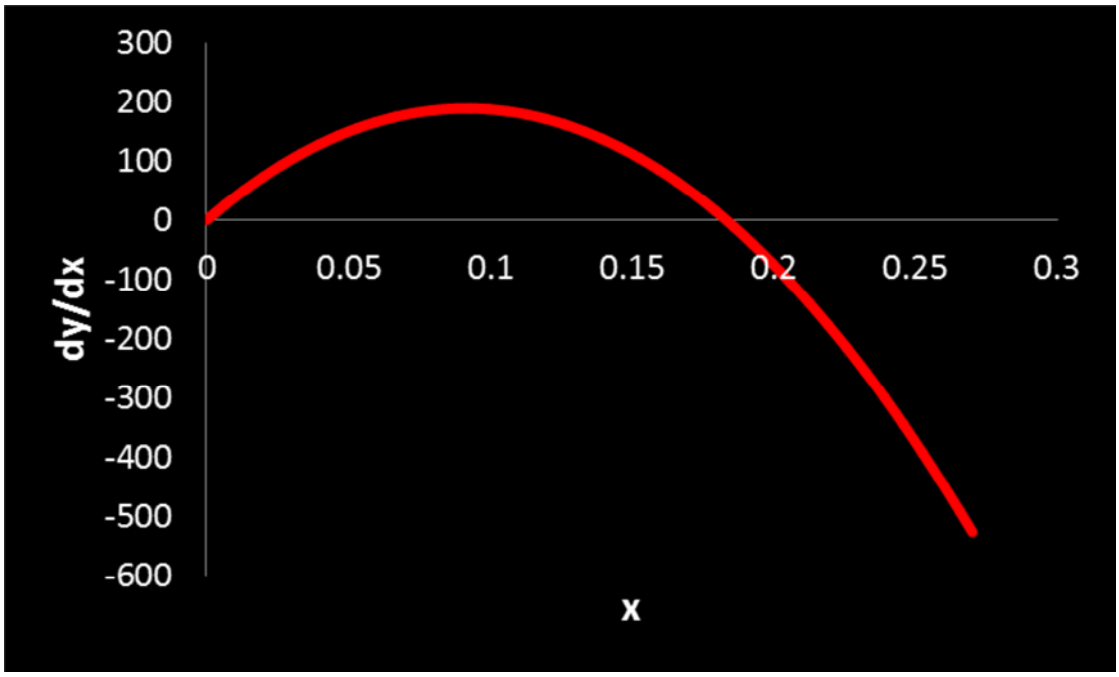

Fig. 12. First derivative of P-ω equation.

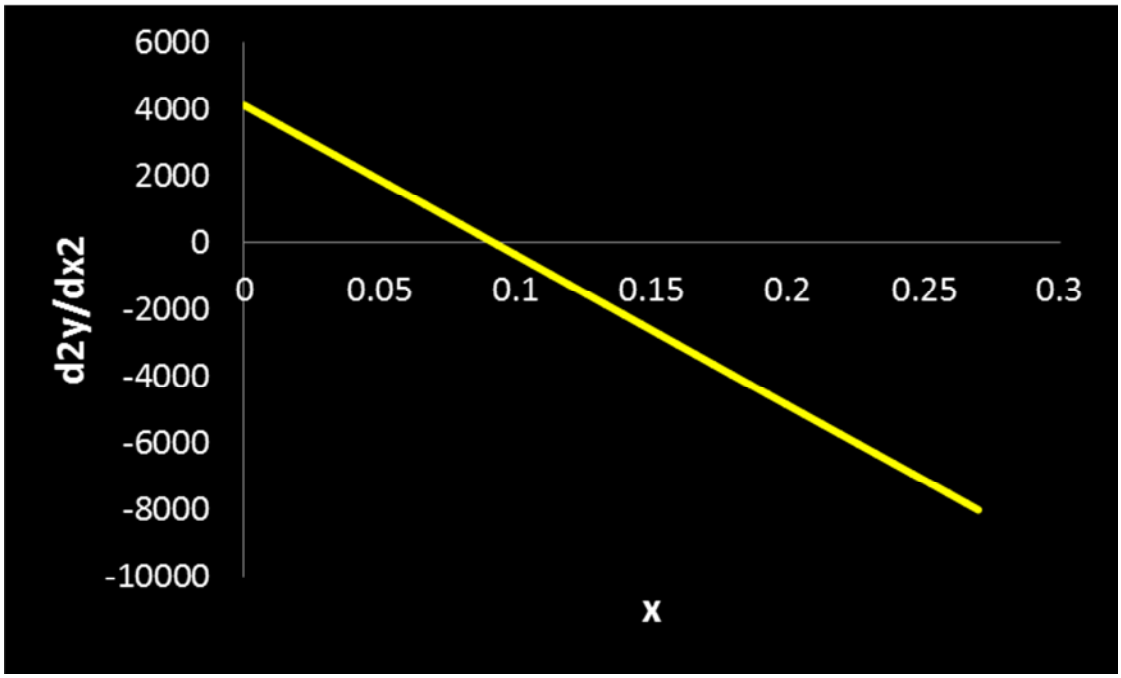

Fig. 13. Second derivative of P-ω equation.

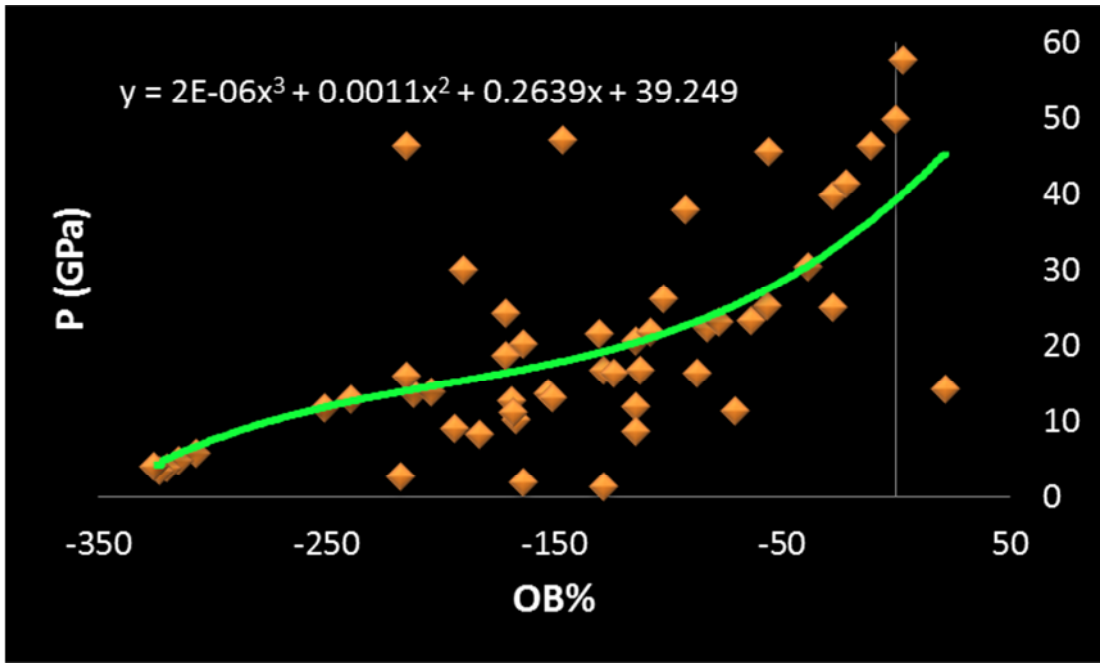

Fig. 14. Comparison of the P (pressure of detonation) values of the tetrahedrane derivatives influenced by the oxygen balance of substituents.

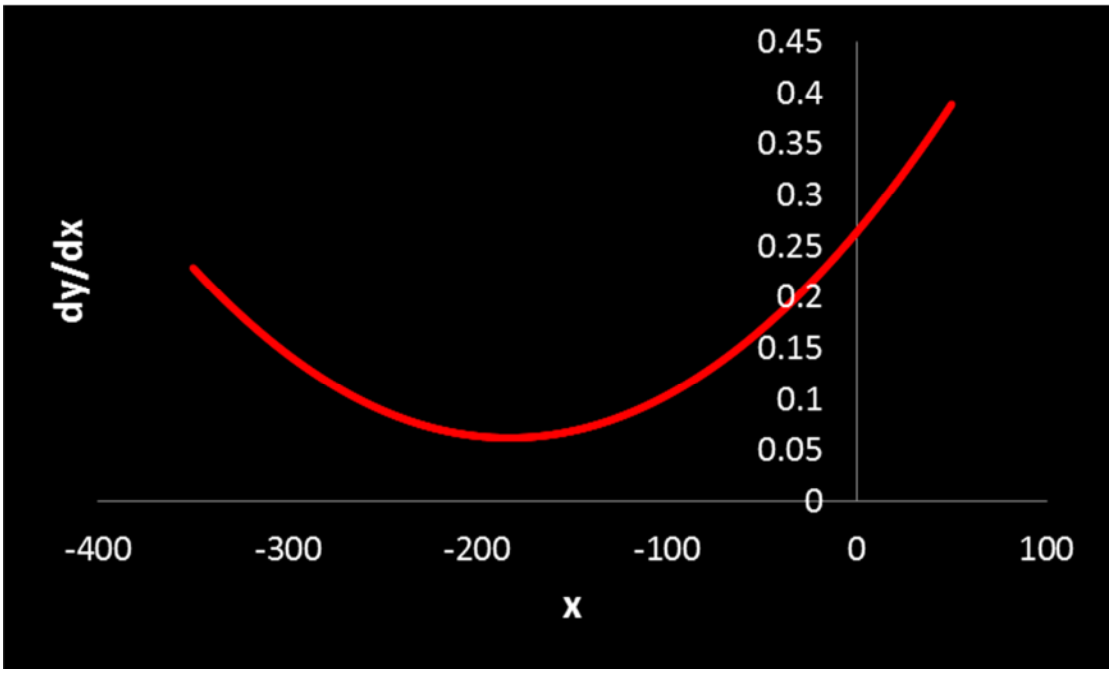

Fig. 15. First derivative of P-OB_{100} equation.

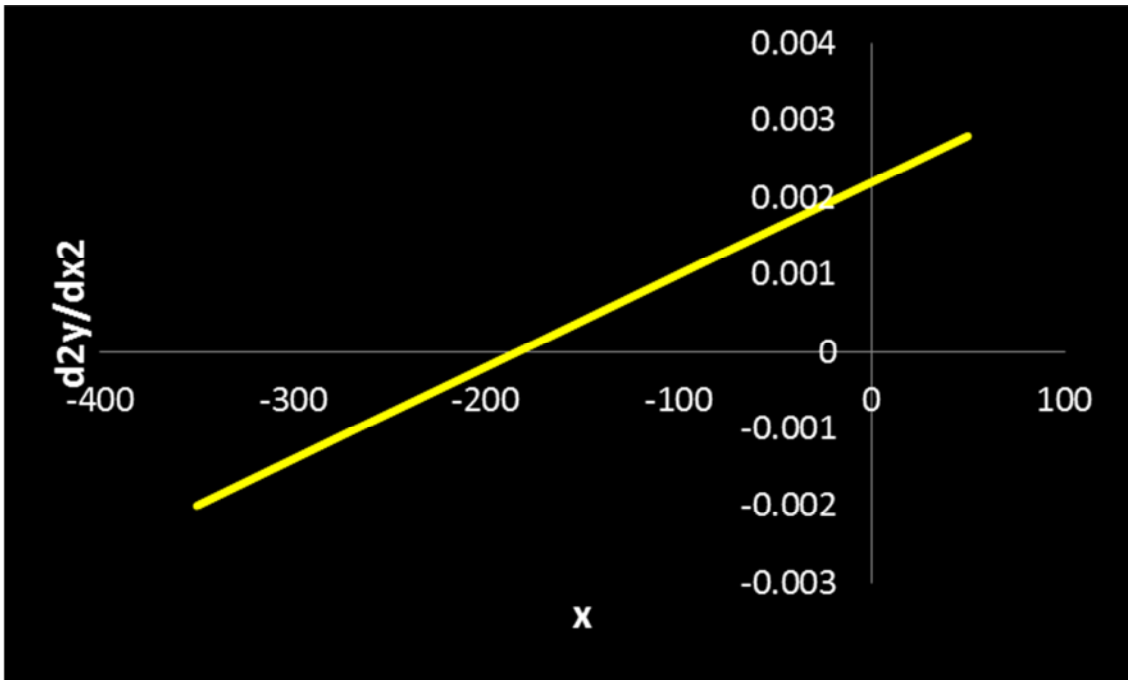

Fig. 16. Second derivative of P-OB_{100} equation.

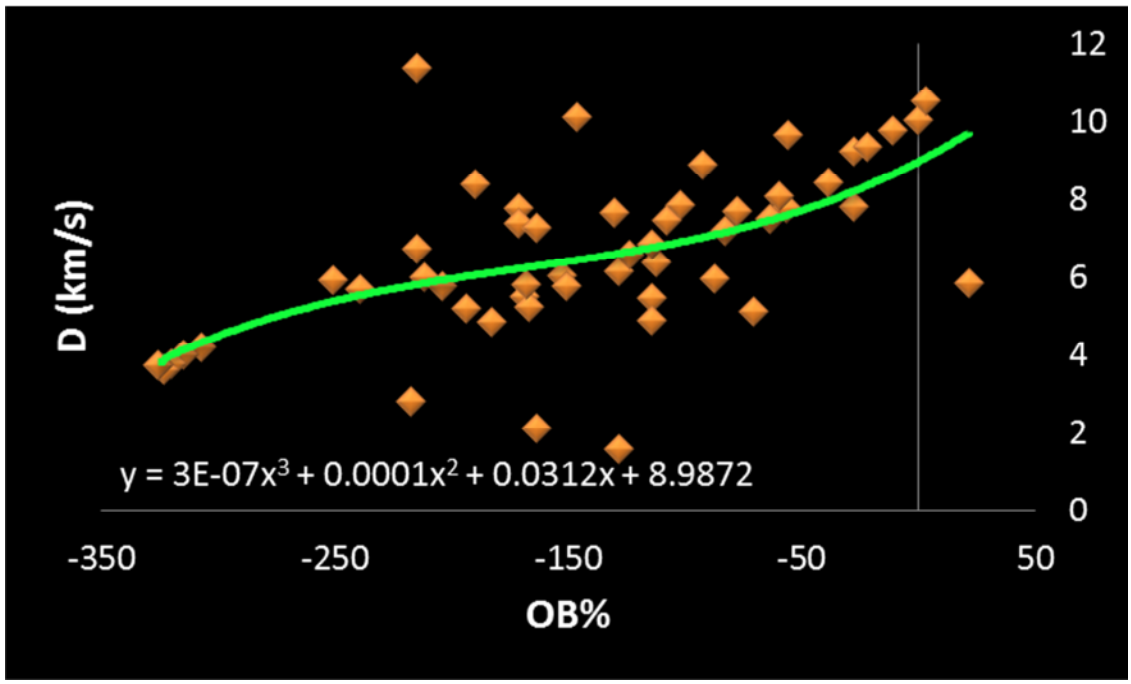

Fig. 17. Comparison of the D (velocity of detonation) values of the tetrahedrane derivatives influenced by the oxygen balance of substituents.

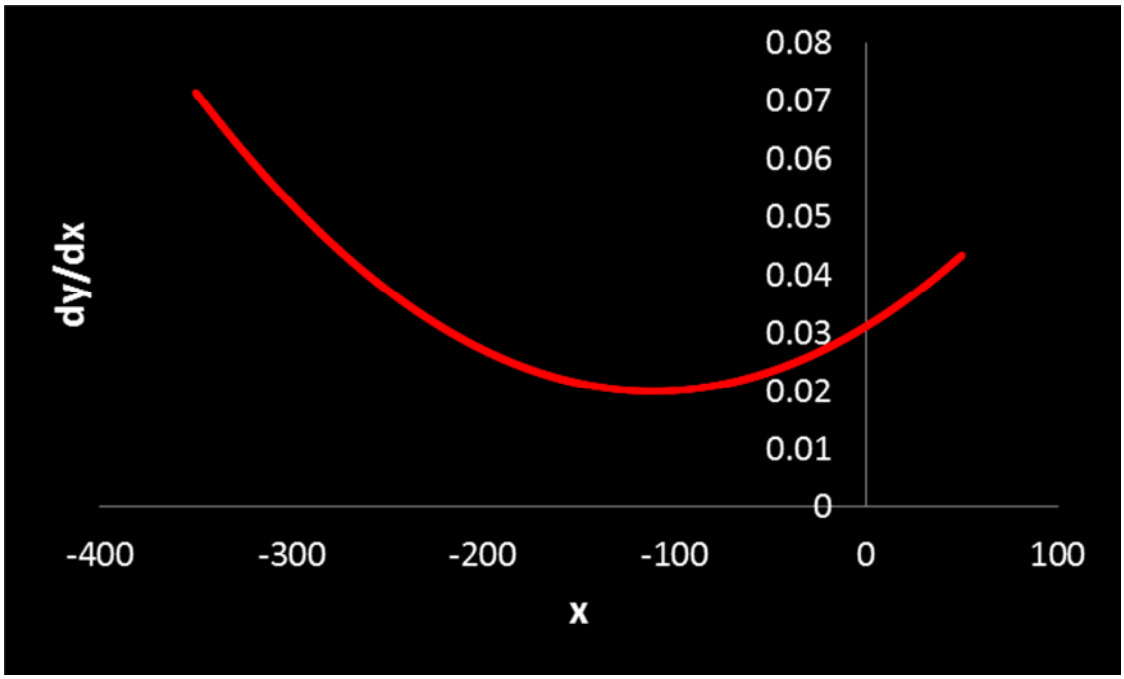

Fig. 18. First derivative of D-OB$_{100}$ equation.

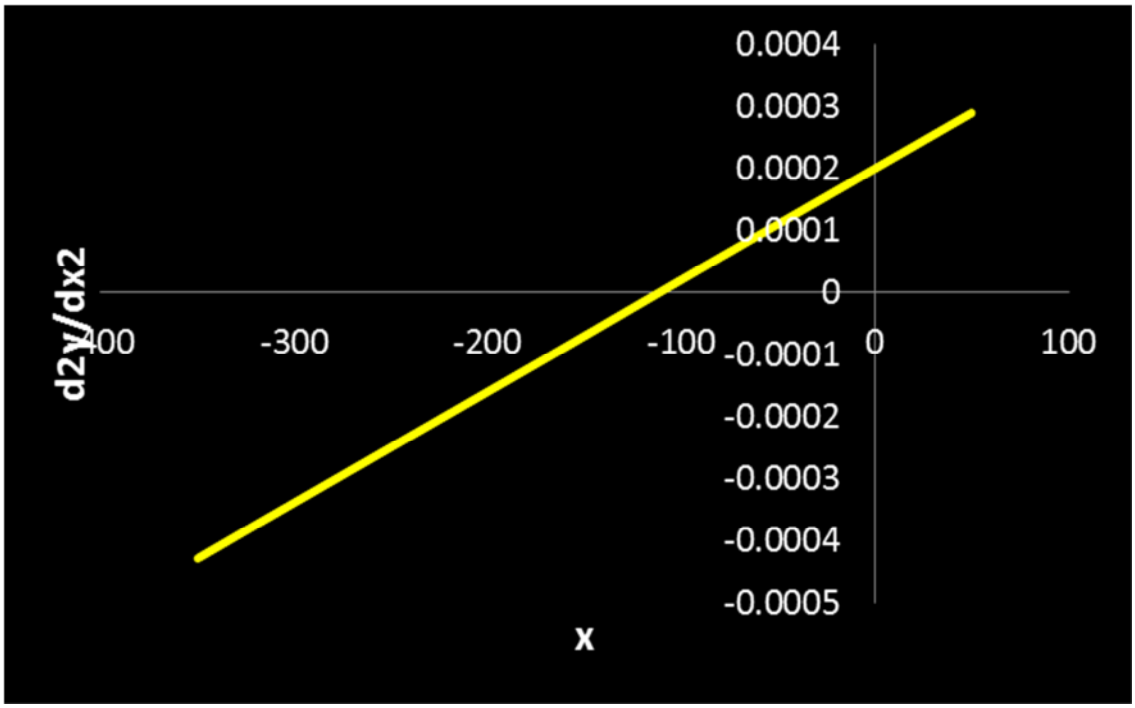

Fig. 19. Second derivative of D-OB$_{100}$ equation

Table 1. The Mulliken atomic charges of the structures

Structures	Charge on $C_{tetrahedrane}$ attached to H (e)	Charge on $C_{tetrahedrane}$ attached to R (e)
Tetrahedrane	C1,C2,C3,C4(-0.144)	-
A1	C2,C3,C4(-0.174)	C1(0.159)
A2	C3,C4(-0.205)	C1,C2(0.130)
A3	C4(-0.237)	C1,C2,C3(0.100)
A4	-	C1,C2,C3,C4(0.070)
B1	C2,C3,C4(-0.170)	C1(0.274)
B2	C3,C4(-0.198)	C1,C2(0.257)
B3	C4(-0.230)	C1,C2,C3(0.240)
B4	-	C1,C2,C3,C4(0.070)
C1	C2(-0.151); C3,C4(-0.174)	C1(0.249)
C2	C3(-0.162); C4(-0.211)	C1,C2(0.229)
C3	C4(-0.188)	C1(0.157); C2(0.268); C3(0.089)
C4	-	C1,C2(0.100); C3,C4(0.239)
D1	C2,C3,C4(-0.138)	C1(0.185)
D2	C3,C4(-0.131)	C1,C2(0.199)
D3	C4(-0.124)	C1,C2,C3(0.216)
D4	-	C1,C2,C3,C4(0.0.237)
E1	C2(-0.170); C3,C4(-0.136)	C1(0.121)
E2	C3(-0.161); C4(-0.174)	C1,C2(0.126)
E3	C4(-0.148)	C1(0.104); C2(0.111); C3(0.082)
E4	-	C1(0.075); C2(0.081); C3(0.083); C4(0.089)
F1	C2(-0.135); C3(-0.137); C4(-0.202)	C1(0.068)
F2	C3(-0.147); C4(-0.205)	C1(0.008); C2(0.075)
F3	C4(-0.243)	C1(-0.104); C2(0.072); C3(0.073)
F4	-	C1(-0.027); C2(-0.002); C3(0.011); C4(0.059)
G1	C2,C4(-0.156); C3(-0.200)	C1(0.213)
G2	C3(-0.173); C4(-0.205)	C1(0.182); C2(0.201)
G3	C4(-0.252)	C1(0.167); C2(0.188); C3(0.191)
G4	-	C1,C3(0.073); C2(0.058); C4(0.151)
H1	C2(-0.205); C3(-0.250); C4(-0.267)	C1(0.303)
H2	C3(-0.124); C4(-0.225)	C1(0.249); C2(0.252)
H3	C4(-0.265)	C1(0.208); C2(0.253); C3(0.312)
H4	-	C1(-0.064); C2(0.353); C3(0.211); C4(0.362)
I1	C2(-0.173); C3(-0.143); C4(-0.116)	C1(0.284)
I2	C3(-0.190); C4(-0.081)	C1(0.287); C2(0.288)
I3	C4(-0.168)	C1(0.245); C2(0.304); C3(0.359)
I4	-	C1(0.260); C2(0.272); C3(0.303); C4(0.331)
J1	C2,C3(-0.120); C4(-0.127)	C1(0.265)
J2	C2(-0.106); C4(-0.105)	C1,C3(0.211)
J3	C4(-0.077)	C1,C3(0.218); C2(0.251)
J4	-	C1,C2,C3,C4(0.247)
K1	C2(-0.136); C3(-0.127); C4(-0.118)	C1(0.230)
K2	C3(-0.110); C4(-0.100)	C1,C2(0.210)
K3	C4(-0.099)	C1(0.211); C2(0.216); C3(0.217)
K4	-	C1,C2,C3,C4(0.220)
L1	C2,C3(-0.141); C4(-0.165)	C1(0.310)
L2	C3(-0.157); C4(-0.135)	C1(0.288); C2(0.317)
L3	C4(-0.126)	C1,C2,C3(0.299)
L4	-	C1(0.315); C2(0.317); C3(0.376); C4(0.385)
M1	C2,C3,C4(-0.145)	C1(0.314)
M2	C3(-0.166); C4(-0.156)	C1,C2(0.259)
M3	C4(-0.168)	C1,C2,C3(0.256)
M4	-	C1,C2,C3,C4(0.205)

Table 2. The frontier orbitals energy of the structures calculated at B3LYP/6-31G(d) level

Structures	ε_{HOMO} (a.u.)	ε_{LUMO} (a.u.)	μ (a.u.)	(a.u.)	ω (a.u.)
Tetrahedrane	-0.22038	0.11982	0.050280	0.34020	0.00372
A1	-0.21149	0.11384	0.048825	0.32533	0.00366
A2	-0.20307	0.10753	0.047770	0.31060	0.00367
A3	-0.19550	0.10017	0.047665	0.29567	0.00384
A4	-0.18821	0.09231	0.047950	0.28052	0.00410
B1	-0.22479	0.09074	0.067025	0.31553	0.00712
B2	-0.22655	0.05586	0.085345	0.28241	0.01290
B3	-0.23081	0.02063	0.105090	0.25144	0.02196
B4	-0.23205	-0.01232	0.122185	0.21973	0.03397
C1	-0.20335	0.06417	0.069590	0.26752	0.00905
C2	-0.19235	0.04772	0.072315	0.24007	0.01089
C3	-0.19101	-0.03754	0.114275	0.15347	0.04255
C4	-0.18381	-0.02382	0.103815	0.15999	0.03368
D1	-0.25586	0.01664	0.119610	0.27250	0.02625
D2	-0.28251	-0.03797	0.160240	0.24454	0.05250
D3	-0.30382	-0.06937	0.186595	0.23445	0.07425
D4	-0.32093	-0.08823	0.204580	0.23270	0.08993
E1	-0.23780	-0.00067	0.119235	0.23713	0.02998
E2	-0.24992	-0.04105	0.145485	0.20887	0.05067
E3	-0.25830	-0.05223	0.155265	0.20607	0.05849
E4	-0.26323	-0.06225	0.162740	0.20098	0.06589
F1	-0.23061	0.02126	0.104675	0.25187	0.02175
F2	-0.23786	-0.00166	0.119760	0.23620	0.03036
F3	-0.24659	-0.02340	0.134995	0.22319	0.04083
F4	-0.25156	-0.03056	0.141060	0.22100	0.04502
G1	-0.19068	0.08134	0.054670	0.27202	0.00549
G2	-0.17578	0.07097	0.052405	0.24675	0.00556
G3	-0.16210	0.06123	0.050435	0.22333	0.00569
G4	-0.13651	0.01003	0.063240	0.14654	0.01365
H1	-0.30240	0.22087	0.040765	0.52327	0.00159
H2	-0.17478	0.06601	0.054385	0.24079	0.00614
H3	-0.16260	0.06286	0.049870	0.22546	0.00552
H4	-0.12002	0.00999	0.055015	0.13001	0.01164
I1	-0.23190	-0.05072	0.141310	0.18118	0.05511
I2	-0.23792	-0.06389	0.150860	0.17403	0.06539
I3	-0.24800	-0.08406	0.166030	0.16394	0.08407
I4	-0.25916	-0.09520	0.177180	0.16396	0.09562
J1	-0.26076	-0.07207	0.166415	0.18869	0.07338
J2	-0.28001	-0.12125	0.200630	0.15876	0.12677
J3	-0.30858	-0.15077	0.229675	0.15781	0.16713
J4	-0.33035	-0.17495	0.252650	0.15540	0.20538
K1	-0.21284	-0.07265	0.142745	0.14019	0.07219
K2	-0.23614	-0.11326	0.174700	0.12288	0.12419
K3	-0.25696	-0.15608	0.206520	0.10088	0.21139
K4	-0.27087	-0.17086	0.220865	0.10001	0.24388
L1	-0.23940	-0.07243	0.155915	0.16697	0.07280
L2	-0.24876	-0.08640	0.167580	0.16236	0.08648
L3	-0.25252	-0.09524	0.173880	0.15728	0.09612
L4	-0.26673	-0.12556	0.196145	0.14117	0.13626
M1	-0.21646	0.01479	0.100835	0.23125	0.02198
M2	-0.21270	-0.04659	0.129645	0.16611	0.05059
M3	-0.22424	-0.05546	0.139850	0.16878	0.05794
M4	-0.21306	-0.04243	0.127745	0.17063	0.04782

Table 3. Total energy, HOF, predicted density and detonation properties of structures

Structures	Formula	Molecular Mass (amu.)	energy (hartrees)	OB_{100}	HOF (kJ/mol)	Q (kJ/g)	V* (cm^3/mol)	ρ (g/cm^3)	D (km/s)	P (GPa)
Tetrahedrane	C_4H_4	52.03130	-154.576791	-307.51	582.897	2677.474	45.667	1.139	4.202	5.685
A1	C_5H_6	66.04695	-193.870067	-314.93	554.263	2005.676	63.954	1.033	4.014	4.783
A2	C_6H_8	80.06260	-233.162967	-319.75	526.615	1572.033	84.901	0.943	3.763	3.881
A3	C_7H_{10}	94.07825	-272.455484	-323.14	499.973	1270.151	102.027	0.922	3.635	3.548
A4	C_8H_{12}	108.09390	-311.747537	-325.64	474.550	1049.249	106.913	1.011	3.727	4.049
B1	C_4H_3F	70.02188	-253.795166	-217.08	443.467	1513.651	57.658	1.214	2.827	2.706
B2	$C_4H_2F_2$	88.01246	-353.010371	-163.61	312.360	848.222	55.135	1.596	2.124	1.857
B3	C_4HF_3	106.00303	-452.222191	-128.30	190.140	428.701	42.669	2.484	1.587	1.328
B4	C_4F_4	123.99361	-551.430594	-103.23	76.892	148.211	61.453	2.018	-	-
C1	C_4H_4O	68.02621	-229.770327	-211.68	407.792	2282.389	48.433	1.405	6.017	13.661
C2	$C_4H_4O_2$	84.02113	-304.962205	-152.34	237.040	2050.110	60.738	1.383	6.043	13.626
C3	$C_4H_4O_3$	100.01604	-380.194021	-111.98	-38.570	1533.823	63.350	1.579	6.397	16.720
C4	$C_4H_4O_4$	116.01096	-455.401421	-82.75	-250.075	1291.965	67.214	1.726	7.178	22.278
D1	C_5H_3N	77.02655	-246.824311	-238.88	703.957	2184.256	50.326	1.531	5.681	12.920
D2	$C_6H_2N_2$	102.02180	-339.063764	-203.88	846.196	1982.330	63.100	1.617	5.761	13.771
D3	C_7HN_3	127.01705	-431.297389	-182.65	1003.737	1888.670	98.002	1.296	4.830	8.303
D4	C_8N_4	152.01230	-523.526642	-168.41	1172.757	1843.857	91.909	1.654	5.501	12.742
E1	$C_5H_4O_2$	96.02113	-343.132159	-166.63	98.095	1448.063	68.604	1.400	5.223	10.269
E2	$C_6H_4O_4$	140.01096	-531.684909	-114.28	-379.834	849.002	90.836	1.541	5.447	11.928
E3	$C_7H_4O_6$	184.00079	-720.236608	-86.96	-855.004	539.966	95.250	1.932	5.948	16.356
E4	$C_8H_4O_8$	227.99062	-908.786151	-70.18	-1324.512	356.118	130.302	1.750	5.123	11.446
F1	C_5H_5NO	95.03711	-323.253212	-193.61	344.993	1475.774	80.538	1.180	5.209	8.986
F2	$C_6H_6N_2O_2$	138.04293	-491.934374	-150.68	94.641	1001.277	91.862	1.503	5.758	13.108
F3	$C_7H_7N_3O_3$	181.04874	-660.610149	-128.14	-141.567	770.873	101.654	1.781	6.154	16.690
F4	$C_8H_8N_4O_4$	224.05455	-829.291215	-114.26	-391.666	614.099	165.731	1.352	4.876	8.729
G1	C_4H_5N	67.04220	-209.901128	-250.59	629.097	2242.679	56.542	1.186	5.929	11.687
G2	$C_4H_6N_2$	82.05310	-265.224887	-214.50	676.814	1971.388	64.583	1.271	6.729	15.883
G3	$C_4H_7N_3$	97.06400	-320.548035	-189.57	726.135	1787.958	57.814	1.679	8.394	29.948
G4	$C_4H_8N_4$	112.07490	-375.905111	-171.31	686.379	1463.704	73.552	1.524	7.788	24.206
H1	$C_4H_6N_2$	82.05310	-263.500482	-214.50	5204.243	15158.647	62.857	1.305	11.393	46.429
H2	$C_4H_8N_4$	112.07490	-375.812979	-171.31	928.271	1979.541	90.112	1.244	7.373	18.756
H3	$C_4H_{10}N_6$	142.09669	-486.429350	-146.38	1105.482	1859.370	74.472	1.908	10.140	47.199
H4	$C_4H_{12}N_8$	172.11849	-597.153602	-130.14	999.451	1387.817	128.016	1.345	7.664	21.481
I1	$C_4H_4N_2O_2$	112.02728	-414.383962	-114.26	491.118	2079.646	63.418	1.766	6.847	20.556
I2	$C_4H_4N_4O_4$	172.02325	-674.187825	-55.81	408.023	1785.616	80.532	2.136	9.654	45.534
I3	$C_4H_4N_6O_6$	232.01923	-933.994195	-27.58	318.346	1636.868	118.499	1.958	9.237	39.743
I4	$C_4H_4N_8O_8$	292.01521	-1193.800756	-10.96	228.168	1548.831	139.161	2.098	9.792	46.395
J1	$C_4H_3NO_2$	97.01638	-359.061224	-123.69	440.720	2221.733	68.702	1.412	6.565	16.324
J2	$C_4H_2N_2O_4$	142.00146	-563.538552	-56.34	317.196	1934.381	87.302	1.627	7.791	25.291
J3	$C_4HN_3O_6$	186.98653	-768.012304	-21.39	203.062	1797.291	92.430	2.023	9.333	41.321
J4	$C_4N_4O_8$	231.97161	-972.481425	0.00	101.086	1725.899	106.112	2.186	10.030	49.743
K1	C_4H_3NO	81.02146	-283.866204	-167.86	619.721	2541.467	67.922	1.193	5.792	11.208
K2	$C_4H_2N_2O_2$	110.01163	-413.151244	-101.81	668.026	2404.140	65.477	1.680	7.836	26.111
K3	$C_4HN_3O_3$	139.00179	-542.430027	-63.31	732.760	1914.331	86.941	1.599	7.516	23.273
K4	$C_4N_4O_4$	167.99195	-671.707566	-38.10	800.759	2258.926	99.051	1.696	8.434	30.429
L1	$C_4H_3NO_3$	113.01129	-434.237188	-92.03	312.364	2051.941	54.821	2.061	8.886	37.841
L2	$C_4H_2N_2O_6$	173.99129	-713.894899	-27.59	47.655	1749.022	109.464	1.589	7.814	25.053
L3	$C_4HN_3O_9$	234.97128	-993.551702	3.40	-214.057	1506.314	97.130	2.419	10.532	57.706
L4	$C_4N_4O_{12}$	295.95127	-1273.422109	21.63	-1036.586	434.044	181.345	1.632	5.835	14.214
M1	$C_4H_3N_3$	93.03270	-318.118637	-163.38	985.335	2531.316	64.786	1.436	7.258	20.187
M2	$C_4H_2N_6$	134.03409	-481.722284	-107.44	1225.515	2185.251	91.219	1.469	7.474	21.748
M3	C_4HN_9	175.03549	-645.293676	-77.70	1550.380	2116.947	119.956	1.459	7.711	23.040
M4	C_4N_{12}	216.03689	-808.742714	-59.25	2196.485	2429.956	142.633	1.515	8.072	25.906

*Average valu from 100 single-point volume calculations at studied levels.

Q: Heat of explosion, V: Volume of explosion, D: Velocity of detonation, P: Pressure of explosion

Table 4. NBO analysis of the tetrahedrane, H1 and H2 structures

Bonds	Occupancy	Population/Bond orbital/Hybrids
C-C (tetrahedrane)	1.96065	50.00% C1 ($SP^{4.08}d^{0.01}$), 50.00% C2 ($SP^{4.08}d^{0.01}$)
C-H (tetrahedrane)	1.99730	63.67% C ($SP^{1.46}$), 36.33% H (S)
C_H-C_{NHNH2} (H1)	1.96224	51.54% C_H ($SP^{3.39}d^{0.01}$), 48.46% C_{NHNH2} ($SP^{3.46}d^{0.01}$)
C_H-C_H (H1)	1.95983	50.46% C ($SP^{4.09}d^{0.01}$), 49.54% C ($SP^{4.18}d^{0.01}$)
C-H (H1)	1.99661	63.35% C ($SP^{1.50}$), 36.65% H (S)
C-N (H1)	1.99309	41.89% C ($SP^{1.89}$), 58.11% N ($SP^{1.97}$)
C_H-C_{NHNH2} (H2)	1.93381	49.37% C_H ($SP^{4.36}d^{0.01}$), 50.63% C_{NHNH2} ($SP^{4.23}d^{0.01}$)
C_H-C_H (H2)	1.95050	50.54% C ($SP^{4.66}d^{0.01}$), 49.46% C ($SP^{4.56}d^{0.01}$)
C-H (H2)	1.99602	63.78% C ($SP^{1.44}$), 36.22% H (S)
C-N (H2)	1.99319	41.79% C ($SP^{1.85}$), 58.21% N ($SP^{1.95}$)

REFERENCES

[1] G. Maier, Angew. Chem. Int. Ed. Engl. 27, (1988) 309.

[2] T. Yildirim, P. M. Gehring, D. A. Neumann, P. E. Eaton and T. Emrick, Carbon 36, (1998) 809.

[3] M. N. Glukhovtsev, S. Laiter and A. Pross, J. Phys. Chem. 99, (1995) 6828.

[4] G. Maier, J. Neudert, O. Wolf, D. Pappusch, A. Sekiguchi, M. Tanaka and T. Matsuo, J. Am. Chem. Soc. 124, (2002) 13819.

[5] H. Kollmar, J. Am. Chem. Soc. 102, (1980) 2617.

[6] A. Sekiguchi and M. Tanaka, J. Am. Chem. Soc. 125, (2003) 12684.

[7] Y. H. Zhang, J. C. Yuan, Y. Q. Yin, Z. Y. Zhou and A. S. C. Chan, Polyhedron 20, (2001) 1859.

[8] M. Mahkam, M. Nabati, A. Latifpour and J. Aboudi, Des. Monomers Polym. 17, (2014) 453.

[9] M. Mahkam, Z. Namazifar, M. Nabati and J. Aboudi, Iran. J. Org. Chem. 6, (2014) 1217.

[10] M. Nabati and M. Mahkam, Iran. Chem. Commun. 2, (2014) 164.

[11] M. Mahkam, H. R. Kafshboran and M. Nabati, Des. Monomers Polym. 17, (2014) 784.

[12] M. Nabati and M. Mahkam, Iran. Chem. Commun. 2, (2014) 129.

[13] M. Nabati and M. Mahkam, Iran. J. Org. Chem. 5, (2013) 1157.

[14] M. Mahkam, M. Nabati and H. R. Kafshboran, Iran. Chem. Commun. 2, (2014) 34.

[15] L. Turker and T. Atalar, J. Hazard. Mater. A 137, (2006) 1333.

[16] M. Nabati, M. Mahkam and H. Heidari, Iran. Chem. Commun. 2, (2014) 236.

[17] B. S. Jursic, J. Mol. Struct. 499, (2000) 137.

[18] M. J. Frisch, G. W. Trucks, H. B. Schlegel, G. E. Scuseria, M. A. Robb, J. R. Cheeseman, J. A. Montgomery Jr., T. Vreven, K. N. Kudin, J. C. Burant, J. M. Millam, S. S. Iyengar, J. Tomasi, V. Barone, B. Mennucci, M. Cossi, G. Scalmani, N. Rega, G. A. Petersson, H. Nakatsuji, M. Hada, M. Ehara, K. Toyota, R. Fukuda, J. Hasegawa, M. Ishida, T. Nakajima, Y. Honda, O. Kitao, H. Nakai, M. Klene, X. Li, J. E. Knox, H. P. Hratchian, J. B. Cross, C. Adamo, J. Jaramillo, R. Gomperts, R. E. Stratmann, O. Yazyev, A. J. Austin, R. Cammi, C. Pomelli, J. W. Ochterski, P. Y. Ayala, K. Morokuma, G.A. Voth, P. Salvador, J. J. Dannenberg, V. G. Zakrzewski, S. Dapprich, A. D. Daniels, M. C. Strain, O. Farkas, D. K. Malick, A. D. Rabuck, K. Raghavachari, J. B. Foresman, J. V. Ortiz, Q. Cui, A. G. Baboul, S. Clifford, J. Cioslowski, B.

B. Stefanov, G. Liu, A. Liashenko, P. Piskorz, I. Komaromi, R. L. Martin, D. J. Fox, T. Keith, M. A. Al-Laham, C. Y. Peng, A. Nanayakkara, M. Challacombe, P. M. W. Gill, B. Johnson, W. Chen, M. W. Wong, C. Gonzalez and J. A. Pople, Gaussian 03. Revision B.01. Gaussian Inc. Wallingford. CT. 2004.

[19] S. H. Vosko, L. Wilk and M. Nusair, Can. J. Phys. 58, (1980) 1200.

[20] C. Lee, W. Yang and R. G. Parr, Phys. Rev. B 37, (1988) 785.

[21] B. Miehlich, A. Savin, H. Stoll and H. Preuss, Chem. Phys. Lett. 157, (1989) 200.

[22] M. Nabati and M. Mahkam, Silicon 7, (2016) in press.

[23] N. Saikia and R. C. Deka, Chem. Phys. Lett. 500, (2010) 65.

[24] R. Parr and R. G. Pearson, J. Am. Chem. Soc. 105, (1983) 7512.

[25] M. Nabati and M. Mahkam, Iran. J. Org. Chem. 6, (2014) 1331.

[26] R. G. Parr, L. V. Szentpaly and S. Liu, J. Am. Chem. Soc. 121, (1999) 1922.

[27] A. Teymori, S. Amiri, B. Massoumi, M. Mahkam and M. Nabati, Iran. J. Org. Chem. 6, (2014) 1287.

[28] M. J. Kamlet and S. J. Jacobs, J. Chem. Phys. 48, (1968) 23.

[29] M. Nabati and M. Mahkam, J. Phys. Theor. Chem. IAU Iran 12, (2015) 33.

[30] M. Nabati and M. Mahkam, Iran. J. Org. Chem. 6, (2014) 1397.